Scaffoldless tissue-engineered nerve conduit promotes peripheral nerve regeneration and functional recovery after tibial nerve injury in rats

Aaron M. Adams[1], Keith W. VanDusen[1], Tatiana Y. Kostrominova[3], Jacob P. Mertens[1], Lisa M. Larkin[1, 2, *]

1 Department of Molecular and Integrated Physiology, University of Michigan, Ann Arbor, MI, USA
2 Department of Biomedical Engineering, University of Michigan, Ann Arbor, MI, USA
3 Department of Anatomy and Cell Biology, Indiana University School of Medicine, Northwest, Gary, IN, USA

Abstract

Correspondence to:
Lisa M. Larkin, Ph.D.,
llarkin@umich.edu.

orcid:
0000-0003-0538-1060
(Lisa M. Larkin)

Damage to peripheral nerve tissue may cause loss of function in both the nerve and the targeted muscles it innervates. This study compared the repair capability of engineered nerve conduit (ENC), engineered fibroblast conduit (EFC), and autograft in a 10-mm tibial nerve gap. ENCs were fabricated utilizing primary fibroblasts and the nerve cells of rats on embryonic day 15 (E15). EFCs were fabricated utilizing primary fibroblasts only. Following a 12-week recovery, nerve repair was assessed by measuring contractile properties in the medial gastrocnemius muscle, distal motor nerve conduction velocity in the lateral gastrocnemius, and histology of muscle and nerve. The autografts, ENCs and EFCs reestablished 96%, 87% and 84% of native distal motor nerve conduction velocity in the lateral gastrocnemius, 100%, 44% and 44% of native specific force of medical gastrocnemius, and 63%, 61% and 67% of native medial gastrocnemius mass, respectively. Histology of the repaired nerve revealed large axons in the autograft, larger but fewer axons in the ENC repair, and many smaller axons in the EFC repair. Muscle histology revealed similar muscle fiber cross-sectional areas among autograft, ENC and EFC repairs. In conclusion, both ENCs and EFCs promoted nerve regeneration in a 10-mm tibial nerve gap repair, suggesting that the E15 rat nerve cells may not be necessary for nerve regeneration, and EFC alone can suffice for peripheral nerve injury repair.

Key Words: nerve regeneration; peripheral nerve repair; neural conduit; tissue engineering; fibroblasts; neural cells

Introduction

Damage to peripheral nerve tissue may cause loss of function in both the nerve and the targeted muscles it innervates. Exposure and direct attachment of healthy nerve tissue on either side of the damaged site allows for optimal outcomes; however, large injuries prohibit tension-free direct repairs (Ray and Mackinnon, 2010). Such cases require tissue replacement to bridge the gap and allow for neural regeneration (Lundborg et al., 1982; Wood et al., 2010). The host-derived autograft is currently the "gold standard" for peripheral nerve repair, providing a bridge for regenerating axons similar to the damaged nerve (Schmidt and Leach, 2003; Meek et al., 2004). However, autograft repairs are limited due to the finite amount of donor nerve tissue available, as well as the potential for neuroma, loss of function, and scarring at the donor site (Millesi, 1990, 2007; Taras et al., 2005).

Due to the limitations associated with autografts, considerable research has been devoted to the design of graft alternatives, such as engineered conduits, to bridge damaged nerve gaps. Unlike autografts, biological and synthetic conduits are not limited by availability, donor site morbidity, or the need for multiple surgical procedures (Taras et al., 2005). In general, engineered conduits have an exterior scaffold and often have a neurotrophic growth factor or cell suspension in the center. The scaffold provides a guide for regenerating axons to migrate toward target tissues and prevent neuronal sprouting, which occurs when axons grow out of the conduit and may result in neuroma formation. The growth factors or cell suspensions enhance nerve regeneration within the scaffold. Scaffolds must also allow for the passage of nutrients and support cells in contact with the regenerating axons. At the same time, scaffolds must inhibit the infiltration of fibroblasts, which may form scar tissue at the injury sites (Schlosshauer et al., 2006; Deumens et al., 2010).

Biological conduits have been fabricated from acellularized and fresh tissues such as skeletal muscle, blood vessels, tendon fibers, and epineurial sheaths (Brandt et al., 1999; Karacaoglu et al., 2001; Risitano et al., 2002; Meek et al., 2004; Maurer et al., 2007). While some of these biological alternatives have been successfully used to bridge a critical gap and allow for nerve regeneration *in vivo*, all are limited by their donor tissue availability and donor site morbidity. These alternatives may provide additional tissues for potential nerve repair, but they do not fully overcome the limitations associated with a nerve autograft.

Synthetic conduits have been engineered from silicones,

poly(lactic-co-glycolic acid) (PLGA), poly-glycolic acid (PGA), polyphosphoester (PPE), and hydrogels (Matsumoto et al., 2000; Wang et al., 2001; Dalton et al., 2002; Toba et al., 2002; Bini et al., 2004; Lundborg, 2004; Kemp et al., 2009).

Synthetic conduits are preferred because they can be fabricated beforehand to accommodate a specific injury (i.e., length of injury site, thickness needed to apply to native nerve stump). Synthetic conduits are designed to accommodate specific environments in regard to porosity, biodegradability, and biocompatibility (Larkin et al., 2006). Despite the benefits that a synthetic scaffold may possess, they most often require incorporation of an inner matrix material to assist and guide axonal regeneration and have a potential for material bioincompatibility (Deumens et al., 2010).

Additionally, the scaffold itself can be a source of mechanical restrain and poor cell adhesion. Scaffolds can be incorporated with nerve-compatible biomaterials, neurotrophic factors, and/or support cells. Common biomaterials incorporated into conduits include collagen, fibronectin, laminin, alginate, silk, Matrigel, and fibrin (Archibald et al., 1991; Akassoglou et al., 2002; Verdu et al., 2002; Yang et al., 2007; Alluin et al., 2009). These materials have all demonstrated an allowance for increased axonal regeneration and can provide an adherent substance on which regenerating nerve may migrate. Neurotrophic factors such as glial-derived neurotrofic factor (GDNF) and nerve growth factor (NGF) as well as Schwann cells and stem cells have been supplemented into conduits to enhance neural regeneration toward targeted tissues (Hudson et al., 2000; Lee et al., 2003; Wood et al., 2009; Lopatina et al., 2011).

Our laboratory has fabricated scaffoldless three-dimensional (3D) engineered nerve conduits (ENCs) from fibroblast monolayers co-cultured with E15 spinal cord-derived neural stem cells (Baltich et al., 2010). We hypothesized that integrating a network of these cells into a conduit would offer several advantages over current technologies. Previous studies have demonstrated the potential of neural stem cells to aid in peripheral nerve regeneration (Murakami et al., 2003; Heine et al., 2004). This is hypothesized to be due in part to the cellular release of neurotrophic factors, including brain-derived neurotrophic factor (BNGF), and GDNF, which have been demonstrated to improve motor axon regeneration (Boyd and Gordon, 2003). By incorporating neural stem cells into our conduit, we hoped to provide a sustained release of neurotrophic factors at physiologically appropriate concentrations. Neural progenitors have been demonstrated to alter the structure of their surrounding extracellular matrix, rendering it more favorable for axonal growth (Zuo et al., 2002). Thus, we hypothesized that incorporating these cells in our ENC will also optimize its architecture for enhancing nerve regeneration. Our scaffoldless approach avoids the limitations associated with scaffold technologies, including incompatibility with the host environment, failure to replicate the native tissues' mechanical and structural properties, and inhibition of nutrient exchange. Furthermore, the ENC is fabricated from a stem cell source, allowing the conduit to be host-derived without the

limitation of donor-site morbidity.

The purpose of this study was to evaluate the repair capabilities of our scaffoldless 3D ENCs in a 10-mm nerve gap in the tibial nerve of adult Fisher F344 rats. A 10-cm segment of tibial nerve was axotomized, denervating both the medial and lateral gastrocnemius muscles. The resulting nerve gap was repaired using an ENC, an engineered fibroblast conduit (EFC), or a reversed nerve autograft. After 12 weeks, we assessed the recovery by measuring the contractile properties in the medial gastrocnemius muscle. Histological analyses of the autograft, ENC, and EFC were performed to assess nerve regeneration with respect to axon count and diameter. Muscle fiber cross-sectional area and central nucleation percent were measured using hematoxylin-eosin and laminin/4′,6-diamidino-2-phenylindole (DAPI) immunohistochemistry.

Materials and Methods
Animals
Twenty-three female Fischer 344 retired breeder rats (3–4 months of age) (Charles River Laboratories, Wilmington, MA, USA) were used either to obtain fibroblasts ($n = 2$) or to undergo nerve repair surgeries ($n = 21$). On embryonic day 15 (E15), fetal rats from pregnant Fischer 344 retired breeder rats ($n = 2$) (Charles River Laboratories) were used to obtain nerve cells. All rats were acclimated to 12-hour light/dark light cycle at 25°C, and *ad libitum* feeding schedule was established in our animal colony for 1 week prior to either surgery or tissue harvesting. All animal care and animal surgeries were performed in accordance with the Guide for Care and Use of Laboratory Animals (Public Health Service, 19965, NIH Publication No. 85-23) and the protocol (09512) was approved by the University Committee for the Use and Care of Animals.

Preparation of self organized fibroblast monolayer
Primary rat tendon fibroblasts were obtained from the Achilles tendons of F344 rats. Tendons were dissociated in 0.25% trypsin-ethylenediaminetetraacetic acid (EDTA) and collagenase I (Worthington Biochemical, Lakewood, NJ, USA) in Dulbecco's modified Eagle medium (DMEM; Gibco, Carlsbad, CA, USA). The harvested fibroblasts were then seeded in a 100-mm dish in the presence of growth medium (GM, Ham's F12 medium (Gibco, Grand Island, NY, USA)), 20% fetal bovine serum (FBS; Gibco), 1% antibiotic-antimycotic (ABAM; Gibco), supplemented with 2.52 ng/mL basic fibroblast growth factor (bFGF) and allowed to expand until confluent. Once confluent, fibroblasts were lifted from the expansion plates using 0.25% trypsin-EDTA and seeded at 20% density in a new 100-mm dish. Cells were repeatedly passaged to reestablish confluence. Fibroblasts to be used for experiments were seeded into three 100-mm dishes and treated with GM supplemented with 2.52 ng/mL bFGF and 200 ng/mL L-ascorbic acid 2-phosphate (Sigma-Aldrich, St. Louis, MO, USA) and bFGF (R&D Systems, Minneapolis, MN, USA). Medium was changed every other day until monolayer was confluent, for a minimum of
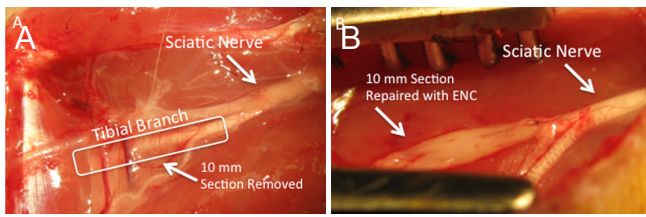
Figure 1 Surgical repair of a 10 mm sciatic nerve gap using EFC and ENC.
(A) 10 mm gaps were surgically created in the tibial nerves of female Fischer 344 rats approximately 5 mm from the site where they innervate the gastrocnemius muscles. Autografts, ENCs, and EFCs were coapted to the nerve stumps as diagrammed to guide nerve regeneration. (B) The grafts were coapted to the nerve stumps of the tibial nerve on either side of the 1 cm acute damage site. An ENC is shown. EFC: Engineered fibroblast conduit; ENC: engineered nerve conduit.

Figure 2 Distal motor nerve conduction velocity after a 12-week recovery.
Values are expressed as the mean ± SEM. *$P < 0.05$, *vs.* control; #$P < 0.05$, *vs.* autograft (one-way analysis of variance followed by Tukey's *post hoc* analysis. In the control group ($n = 5$), the contralateral legs of the autograft animals were used. In the autograft group ($n = 5$), a 10 mm long sciatic nerve segment was transected, reversed, and then coapted to the two newly formed nerve stumps. In the ENC ($n = 8$) and EFC groups ($n = 8$), 10 mm long nerve segments were removed and the engineered conduits were coapted to the distal and proximal nerve stumps. ENC: Engineered nerve conduit; EFC: engineered fibroblast conduit.

5 days. Once confluent, or in GM for 5 days, medium was switched to differentiation medium (DM, including DMEM, 7% horse serum, and 1% ABAM) supplemented with 200 ng/mL L-ascorbic acid 2-phosphate and 0.1 µg/mL transforming growth factor-beta 1 (TGFβ1) (R&D Systems). DM was changed every other day until the plate was switched to serum-free neural basal medium (NBM; Gibco) to form an ENC or until the monolayer spontaneously remodeled under constraints (about 3–5 days) to form an EFC.

Isolation of E15 rat nerve cells
On day E15, fetuses were cesarean delivered from pregnant F344 rats. Fetal spinal cords were dissected out, removing the epithelial covering and tail. Spinal cords were stored in serum-free neurobasal medium (NBM) and then minced using forceps and a razor blade. Minced spinal cord segments were dissociated in serum-free NBM and 0.25% trypsin-EDTA. Dissociation suspensions were strained through a 100 µm cell strainer (Fisher Scientific, Pittsburgh, PA, USA), spun at 1,500 r/min for 10 minutes, and re-suspended in NBM.

Preparation of scaffoldless 3D ENC
Two hundred thousand nerve cells were seeded in NBM on the previously described confluent fibroblast monolayers, removing all serum-containing DM. The plates were fed NBM every other day for the following 7–10 days, until a neural network could be seen. The plates were then treated with GM supplemented with 200 ng/mL L-ascorbic acid 2-phosphate and 2.52 ng/mL bFGF. After 2 days, the plates were treated with DM supplemented with 200 ng/mL L-ascorbic acid 2-phosphate and 0.1 µg/mL TGFβ1. Medium was changed every other day until the monolayer was seen delaminating from the edges of the dish, about 3–4 days after switching to DM. Once the monolayer was released from the dish, it was manually made into a cylinder, and transferred to a sylgard-coated dish (Dow Chemical Corporation, Midland, MI, USA; type 184 silicon elastomer) and held apart 4 cm using constraint pins, where it fused in culture to hold its cylindrical shape. The resulting ENC was 4 cm in length and 2 mm in width, 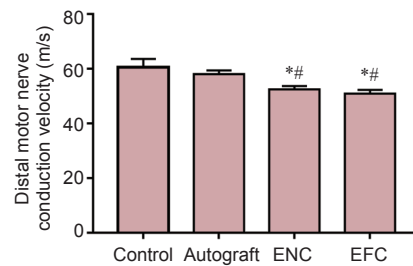and cut to 10 mm lengths to fill the nerve gap. ENCs were fed DM until taut, and then fed GM until implanted. Implantation was performed within 10 days of 3D formation of the conduits.

Preparation of scaffoldless 3D EFC
EFCs were fabricated by forming conduits from fibroblast monolayers without the addition of neuronal cells. EFC monolayers were not fed NBM. Once the EFC monolayers were fed DM they were allowed to delaminate. After the EFC monolayers were released from the dish, they were manually pinned at length on sylgard dishes where they fused into cylinders. The EFCs were fabricated such that the length was 4 cm and the width was 2 mm before being cut to fit the nerve gap. EFCs were fed DM until taut, and then fed with GM until implanted. These tissues did not have hollow centers; the centers were filled with either nerve cells (ENC) or fibroblasts (EFC) and thus would not experience collapse and compression during regeneration.

Surgical procedures
Twenty-one F344 retired breeder rats were anesthetized with Isoflurane and the vastuslateralis and biceps femoris muscles of the left leg were separated to expose the sciatic nerve. The tibial nerve was isolated from the peroneal and sural nerves (**Figure 1A**). The connective tissue was separated from the tibial nerve from the sciatic notch to approximately 3 mm proximal to the site where the nerve innervates the medial and lateral gastrocnemius muscles. Tibial nerve axotomy was performed by transecting the tibial nerve at 15 and 5 mm before its insertion into the gastrocnemius muscles and removing 10 mm long nerve. Animals were divided into three groups. For the autograft control group ($n = 5$), a 10 mm long sciatic nerve segment was transected, reversed and then coapted to the two newly formed nerve stumps using 9-0 silk suture (Ethicon, Cincinnati, OH, US). In the ENC ($n = 8$) and EFC ($n = 8$) groups, following identical removal of 10 mm long nerve segments, engineered conduits were coapted

Table 1 Evaluation of nerve regeneration

	Control (n = 5)	Autograft (n = 5)	ENC (n = 6)	EFC (n = 8)
Axon diameter (μm)	8.72 ± 0.51	7.26 ± 0.38	7.43 ± 0.24	4.62 ± 0.31
Number of axons per 1,000 mm² area	6.47 ± 0.22	10.79 ± 0.36	5.67 ± 0.58	9.70 ± 0.33

Values are presented as the mean ± SEM. Nerve regeneration was measured by total number of myelinated fibers and the mean number of myelinated axons within the graft. Data were obtained utilizing Image J software (National Institutes of Health, Bethesda, MD, USA). Neural cell adhesion molecule and SM312 stained transverse nerve sections were analyzed. In the control group, the contralateral legs of the autograft animals were used. In the autograft group, a 10 mm long sciatic nerve segment was transected, reversed, and then co-apted to the two newly formed nerve stumps. In the ENC and EFC groups, 10 mm long nerve segments were removed and the engineered conduits were coapted to the distal and proximal nerve stumps. ENC: Engineered nerve conduit; EFC: engineered fibroblast conduit.

to the distal and proximal nerve stumps using 9-0 silk suture (**Figure 1B**). Two rats did not recover from anesthesia in the ENC group, reducing the number in this group (*n* = 6). The vastuslateralis and bicepsfemoris muscles were sutured together using 7-0 silk suture (Ethicon), and the skin incision was closed using 9 mm autoclips (Becton Dickinson). Animals were allowed to recover for 12 weeks before the contractile and distal motor response velocity measures were performed and nerve and muscle tissues were harvested to assess the extent of nerve regeneration and the recovery of targeted muscle. In the ENC group, two rats were lost due to anesthetic issues during the surgical procedure, reducing the numbers of animals in this group to six. The contralateral legs of the autograft animals were used as non-surgical controls.

Distal motor nerve conduction velocity

Distal motor nerve conduction velocity was measured according to a previously described method (Maurer et al., 2007). Briefly, rats were anesthetized using sodium pentobarbital (Merck Animal Health, Madison, NJ, USA). The surgery site was reopened by separating the vastuslateralis and biceps femoris muscles and exposing the area of the tibial nerve containing the 10-mm autograft or tissue-engineered conduit. A platinum stimulating electrode of a Viasys TECA Synergy N2 EMG machine (VIASYS Healthcare, Yorba Linda, CA, USA) was placed proximal to the transection site near the sciatic notch. The recording and reference wires were inserted into the lateral gastrocnemius muscle. The tibial nerve was stimulated with EMG settings of 0.3 mA. Distal motor nerve conduction velocity was measured in triplicate while maintaining body and surgical site temperature at 37°C. Stimulation latency was recorded, and the Viasys program was performed to measure distal motor nerve conduction velocity. Distal motor nerve conduction velocities were also recorded on the contralateral tibial nerve and lateral gastrocnemius muscle and used for control measures.

Contractile property measures

Following the motor nerve conduction velocity measures, the medial gastrocnemius muscle was isolated from surrounding muscle and connective tissue. A 4-0 silk suture was tied around the distal tendon, and the tendon was severed distal to the tie. The animal was then placed on a temperature-controlled platform warmed to maintain body temperature at 37°C. The hind limb was immobilized by securing the femur near the knee and clamping the foot to the platform. The distal tendon of the medial gastrocnemius muscle was tied to the lever arm of a servomotor (model 305, Aurora Scientific Inc., Aurora, Ontario, Canada). A constant stream of warm 37°C saline was dripped over the medial gastrocnemius muscle to maintain muscle temperature at 37°C. The medial gastrocnemius muscle was stimulated to contract *via* the tibial nerve proximal to the repair site using a bipolar platinum wire electrode connected to a Grass model S88 stimulator. Data were computed by Labview software (National Instruments, Austin, TX, USA) written specifically for contractile measures. Stimulation voltage and muscle length (Lo) were optimized to produce maximum isometric twitch force. With the muscle held at Lo, trains of stimulus pulses were applied through the tibial nerve at increasing frequencies until maximum isometric tetanic force (Fo) was reached, generally at ~100 Hz. Following the measurements of force in situ, both the experimental and contralateral muscles were removed from the rats, then weighed, flash frozen in TBS medium (Triangle Biological Sciences, Durham, NC, USA), and stored for subsequent histological analysis. Cross-sectional area (CSA) was calculated by dividing the mass of the muscle by the product of fiber length (Lf) and muscle density of 1.06 g/cc. Fo (N) was divided by CSA to obtain the specific force.

Histology

Native nerves (control) from the contralateral side of autograft animals, autografts, ENCs, and EFCs were removed from all animals after distal motor nerve conduction velocities and contractile properties were measured. Due to the work-intensive process of histology, three nerves from each surgical group were randomly chosen for histological analysis. Medial gastrocnemius muscles were dissected from contralateral, autograft, ENC, and EFC hindlimbs. Unfixed samples were placed into TBS medium (Triangle Biological Sciences, Durham, NC, USA), frozen in cold isopentane, and stored at –80°C until needed. Nerve regeneration and muscle structure were analyzed on three specimens from each surgical group. Nerve and muscle tissue samples were cross-sectioned with a cryostat (Thermo-Fischer, Waltham, MA, USA) at a thickness of approximately 12 μm, adhered to Superfrost Plus microscopy slides (Thermo-Fischer, Waltham, MA, USA), and used for staining. Three nerve sections per group were taken at the middle of the repair site and stained with neural cell adhesion molecule to visualize nerve fibers. The entire cross-section for each repair site was analyzed for axon number and axon diameter.

Sections of muscle were stained with hematoxylin and

eosin and the entire cross-section (*n* = 3 per group) was analyzed for signs of muscle denervation, muscle atrophy (CSA), and the number of fibers with central nucleation. For immunohistochemical analysis, frozen muscle and nerve sections were fixed with ice-cold methanol for 10 minutes and rinsed with phosphate buffered saline (PBS). Sections were blocked for 30 minutes with PBS with 0.05% Tween-20 (PBST) containing 20% calf serum (PBST-S) at room temperature. Sections were incubated overnight at 4°C with the primary antibodies diluted in PBST-S. Immunofluorescence staining of the nerve sections with specific antibodies was performed to detect the presence of nerve fibers (rabbit anti-neural cell adhesion molecule (NCAM) polyclonal antibodies, 10 μg/mL, Millipore, Temecula, CA, USA), neurofilament (mouse anti-smooth muscle-312, 1:500, Covance, Emeryville, CA, USA), and skeletal muscle extracellular matrix (Wheat germ agglutinin (WGA) or rabbit anti-laminin polyclonal antibodies, 10 μg/mL, Millipore). Following three washes in PBST, 1-hour incubation with fluorophore-conjugated anti-mouse or anti-rabbit antibody (Jackson ImmunoResearch Laboratory, West Grove, PA, USA) at room temperature was performed for visualization. Following three washes in PBST, co-staining of nerve sections with fluorescein labeled wheat agglutinin (WGA; 5 μg/mL; Molecular Probes, Thermo-Fischer, Waltham, MA, USA) was performed for general visualization of the sample structure. Following three washes in PBST, nuclei were stained by 5 minute incubation with DAPI solution (Sigma, St. Louis, MO, USA) in PBST. The sections were examined and photographed with a Leica microscope (Thermo-Fischer, Waltham, MA, USA).

Statistical analysis

Values are presented as the mean ± SEM. Measurements of significant differences between means were performed using GraphPad Prism 7 (GraphPad Software, Inc., La Jolla, CA, USA). One-way analysis of variance (ANOVA) followed by Tukey's *post hoc* analysis was used to determine the statistical differences among the three repair groups. Resulting differences were considered significant if $P < 0.05$.

Results

Motor nerve conduction velocity

Distal motor nerve conduction velocities of both the ENC and EFC were significantly slower than those of both the contralateral native nerve and autograft. The autograft restored distal motor nerve conduction velocity to 96% of native motor nerve conduction velocity, and that of ENC and EFC dropped to 86.6% and 84.1% of native distal motor nerve conduction velocity, respectively (**Figure 2**).

Muscle contractile properties

After 12 weeks, the medial gastrocnemius muscle in the autograft group recovered 63.1% of native muscle mass, and that in the ENC and EFC groups recovered 41.8% and 37.7% of native muscle mass, respectively (**Figure 3A**). The maximum isometric force produced from the medial gastrocne-mius muscle in the autograft group was 59.8% of native maximum isometric force production (**Figure 3B**), and that in the ENC and EFC groups was 19.8% and 19.7%, respectively. The specific force production (**Figure 3C**) in the autograft group was not statistically different from the native medial gastrocnemius specific force production elicited by the tibial nerve (101% of specific force produced from native medial gastrocnemius muscle). The specific force in the ENC group (43.9% of native) and EFC group (44.1% of native) was significantly less than the autograft and native specific forces (*P* = 0.00056). The muscle masses in the ENC and EFC groups were ~65% of the autograft, and their maximum isometric forces were only ~30% of the autograft isometric force production. This resulted in the specific force production in the ENC and EFC groups being 43% of the specific force of the autograft.

Conduit histology

Immunohistochemical labeling of the grafts with pan-axonal neurofilament marker SM312 revealed neurite growth indicating axonal regeneration 5 mm into the ENC, EFC, and autograft (**Figure 4**). The DAPI counter-staining showed areas of varying cell densities, and higher density corresponded to increased cell division and expansion, which may represent infiltrating support cells as well as fibroblasts. SM312-positive axonal processes were observed throughout the control nerve (**Figure 4**), indicating the presence of intact axonal processes, and few DAPI stained nuclei, which may belong to Schwann cells dispersed within the nerve. The entire cross-section for each repair site was analyzed for axon number and axon diameter. The number of axons per 1,000 μm^2 at the site 5 mm into the graft was found to be greater in the autograft (10.79 ± 0.36) and EFC (9.70 ± 0.33) than in the ENC (5.67 ± 0.58) or non-operated contralateral control (6.47 ± 0.22) (**Table 1**). The diameter of the axons at this point was measured at 85% of the native diameter in the autograft and ENC but only 50% in the EFC repair (**Table 1**).

Muscle histology

Muscle recovery was histologically evaluated by measuring muscle fiber cross-sectional areas and quantifying the percentage of muscle fibers with centralized nuclei (**Figure 5**). The muscle fiber cross-sectional area of the control native medial gastrocnemius muscle was 1,748.53 ± 45.79 μm^2. The average autograft muscle fiber cross-sectional area was decreased by 15% compared to contralateral (control) (1,375.17 ± 149.78 μm^2); the cross-sectional area was decreased by 18% (1,257.35 ± 84.70 μm^2) and 20% in the ENC and EFC groups, respectively compared to control (1,228.90 ± 11.30 μm^2) (**Figure 5I**). All three surgical repair models had a greater percent of centralized nucleation, compared to the 2.0% measured in the non-operated muscle, yet all were less than 10% (**Figure 5J**).

Discussion

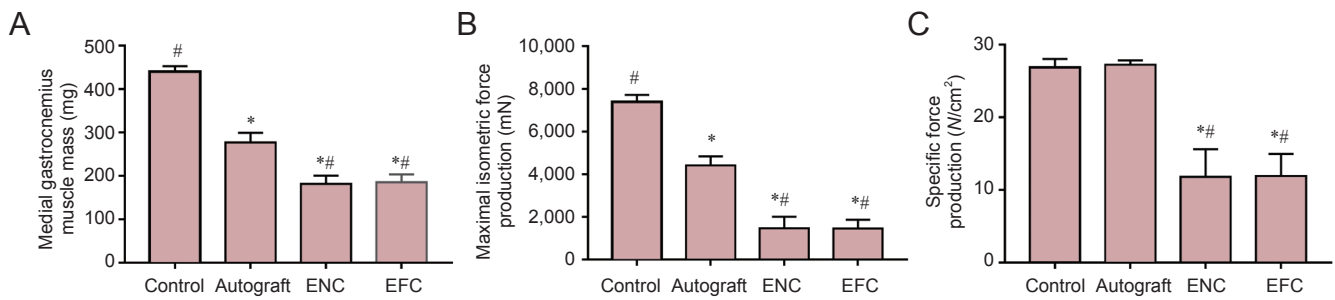In this study, we evaluated the repair capability of ENC in a

Figure 3 Effects of nerve repair on medial gastrocnemius muscle mass (A), maximal isometric force production (B), and specific force production (C) following a 12 week recovery.
Values are expressed as the mean ± SEM. *$P < 0.05$, *vs.* control; #$P < 0.05$, *vs.* autograft (one-way analysis of variance followed by Tukey's *post hoc* analysis). In the control group ($n = 5$ in A–C), the contralateral legs of the autograft animals were used. In the autograft ($n = 5$ in A–C) group, a 10 mm sciatic nerve segment was transected, reversed and then coapted to the two newly formed nerve stumps. In the ENC ($n = 8$ in A, $n = 6$ in B, C) and EFC ($n = 10$ in A, $n = 8$ in B, C) groups, 10 mm nerve segments were removed and the engineered conduits were coapted to the distal and proximal nerve stumps. ENC: Engineered nerve conduit; EFC: engineered fibroblast conduit.
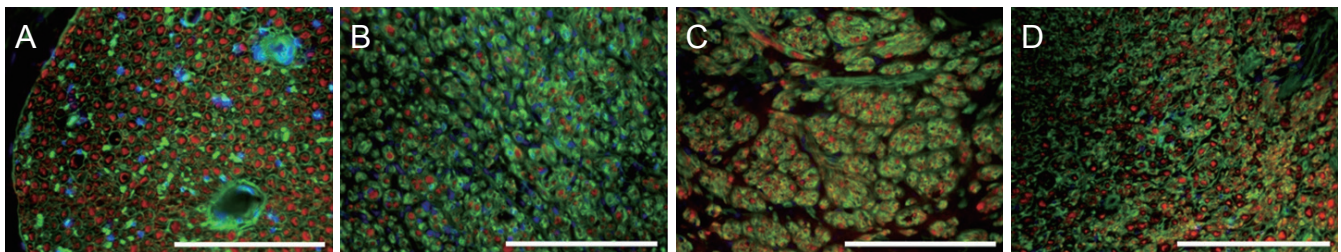

Figure 4 Immunohistochemical staining of transverse sections through native and surgically repaired tibial nerves after 12 weeks of recovery with antibodies against SM312 (red), WGA (connective tissue, green), and DAPI (nuclei, blue).
All sections were taken from the center of the 10 mm repair site. (A) Native tibial nerve from contralateral side which did not undergo axotomy, (B) autograft repaired tibial nerve, (C) ENC repaired tibial nerve, and (D) EFC repaired tibial nerve. Scale bars: 200 μm. ENC: Engineered nerve conduit; EFC: engineered fibroblast conduit; WGA: wheat germ agglutinin; DAPI: 4′,6-diamidino-2-phenylindole.

10-mm long peripheral nerve injury. Our primary objective was to observe if ENC could induce and guide regeneration, such that targeted tissues would be rescued from the denervation-induced atrophy. In this study, we compared the regenerative capability of ENC with that of autografts in the repair of peripheral nerve injuries to find an alternative to autografts. To assess success in nerve regeneration, we analyzed axon counts throughout the nerve repair site. To assess the recovery of our targeted tissue, medial muscle fiber cross-sectional areas and the percentage of centrally nucleated fibers in the medial gastrocnemius muscle were quantified. The maximum and specific force production in the medial gastrocnemius muscle and the distal motor nerve conduction velocity were measured to assess function recovery. Our results revealed that the ENC and fibroblasts-only EFC allowed for nerve regeneration, as evidenced by the presence of axons traversing through the conduit and by the nerve-induced muscle contractions. Abundant robust axons in the autografts may be due to presence of native axonal extracellular matrix (ECM) structure in the autograft tissue, which allows for more efficient neural cell migration during neuronal sprouting. Our results revealed that the ENCs had similarly sized axons as the autografts, but the axon number is smaller, indicating that the ECM of the ENC was sufficient to allow cell migration and neural regeneration, and it was not as good as native ECM. Not surprisingly, the EFC con-

tained more axons than the ENC and native control. Published work from our lab shows that the ECM of an EFC has a highly organized collagen structure, both in cross-section and longitudinally, allowing for cell migration during neuronal sprouting (Mahalingam et al., 2015), however, they were smaller than those of any other group (**Table 1**). It is not known if any of the axons observed in the ENC originated from its isolated E15 nerve cells. Structural organization and axon fiber sizes in the ENC appear similar to those in the non-surgical control, forming perhaps a similar endoneurium compartmentalization around the regenerating nerve fibers (**Figure 2**). Lack of this organization in the EFC may be responsible for the smaller size and ungrouped structure of its axons. Histologically, the ENC allows for similar nerve regeneration to the autograft repair in regard to count, size and organization of axons. Our results demonstrated that the ENC and EFC, however, offered less functional recovery than autograft repair, which could be attributed to a slower rate of nerve regeneration. Many conduit alternatives provided limited functional recovery and conduit alternative incorporating neurotrophic precursor cells can provide better functional recovery. Incorporation of nerve cells isolated from embryonic spinal cord was done to simulate a potential best-case scenario. However, we are now fabricating our ENC from stem cells induced to both a fibroblast and neural lineage. We propose that the ENCs fabricated from primary
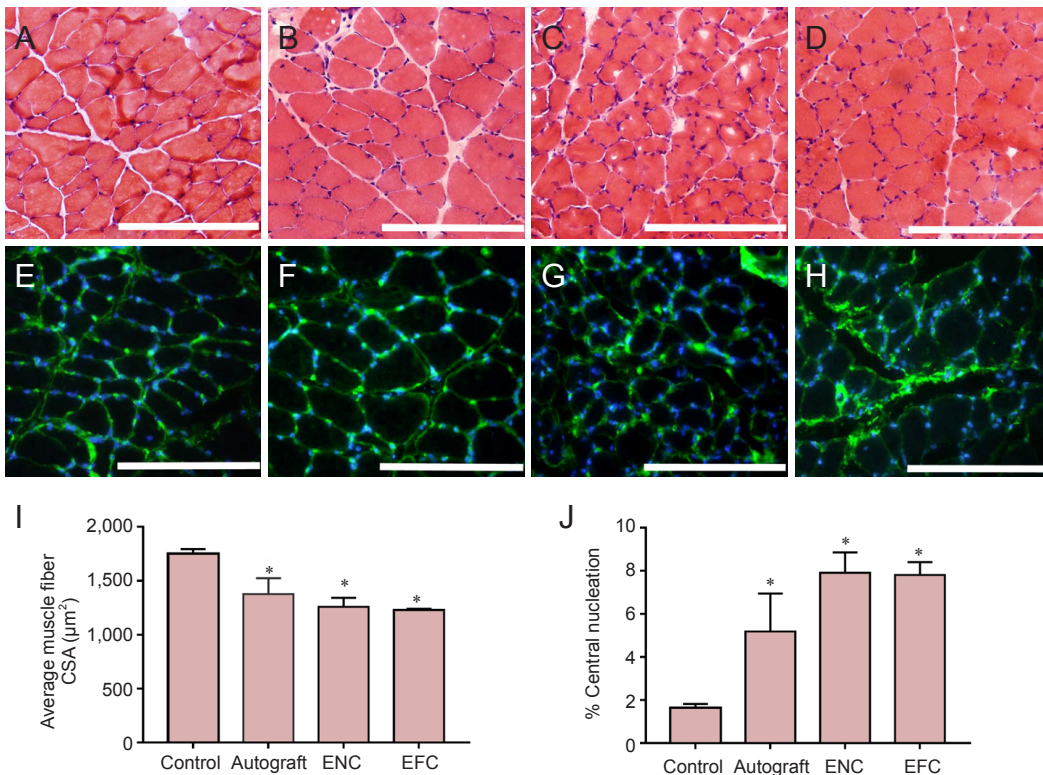
Figure 5 Characterization of structure and nuclei centralization in medial gastrocnemius muscle.
Hematoxylin and eosin staining of the medial gastrocnemius muscle following 12-week recovery in (A) native contralateral leg, (B) autograft, (C) ENC, and (D) EFC repair. Immunohistochemical laminin (green) and nuclei (4′,6-diamidino-2-phenylindole: blue) staining of the medial gastrocnemius muscle in (E) native contralateral leg, (F) autograft, (G) ENC, and (H) EFC repair. Scale bars: 200 μm. Medial gastrocnemius muscle recovery from denervation and atrophy was assessed by (I) muscle fiber cross-sectional area (CSA), and (J) percentage of centrally nucleated fibers. Data regarding laminin and hematoxylin and eosin stained muscle sections were obtained using Image J software. Values are presented as the mean ± SEM from $n = 3$ animals in each group. *$P < 0.05$, *vs*. control (one-way analysis of variance followed by Tukey's *post hoc* analysis). The contralateral legs of the autograft animals ($n = 3$) were used for controls. In the autograft group, a 10 mm long sciatic nerve segment was transected, reversed and then coapted to the two newly formed nerve stumps. In the ENC ($n = 3$) and EFC ($n = 3$) groups, 10 mm long nerve segments were removed and the engineered conduits were coapted to the distal and proximal nerve stumps. ENC: Engineered nerve conduit; EFC: engineered fibroblast conduit.

tendon and spinal cord present a novel technology that is currently being optimized using adult stem cells. After 12 weeks of recovery, we found nearly complete restoration of distal motor nerve conduction velocity in all included groups. Our results showed that distal motor nerve conduction velocity in the autograft group was similar to that in the contralateral side in the other repair groups (58 ± 1.41 m/s *vs*. 60.5 ± 3.11 m/s). The distal motor nerve conduction velocity in the ENC and EFC groups was not completely recovered (52.4 ± 1.31 m/s and 50.9 ± 1.43 m/s), indicating a successful re-establishment of regenerating nerves to the targeted lateral gastrocnemius muscle. After 12 weeks of recovery, the force production successfully recovered in the medial gastrocnemius muscle in the autograft group. While the maximum isometric force was significantly reduced in the autograft group, the specific force of the muscle recovered to the level of native specific force values (27.2 ± 0.64 N/cm² compared to 26.9 ± 1.14 N/cm²). The reduced specific force production in the ENC and EFC groups (11.8 ± 3.82 N/cm² and 11.9 ± 3.07 N/cm²) could have resulted from a reduced rate of nerve regeneration that would have resulted in less time to reestablish

neuromuscular junctions and restore normal muscle function. As expected, the weights of the medial gastrocnemius muscles were 60% lower in the ENC and EFC groups than in the autograft group, which had restored to 60% of the native muscle weight. We compared the percentage of muscle fibers with centralized nuclei in the targeted tissue to measure the recovery of individual muscle fibers from atrophy. Since all three surgical repair groups had less than 10% of their muscle fibers with centralized nuclei, we proposed that each of these groups was able to reestablish a similar number of neuromuscular junctions. Additionally, the fiber cross-sectional areas were equivalent in the autograft, ENC, and EFC groups.

In conclusion, while the nerve regeneration and force production were greater in the autograft group than in the ENC group, the ENC does present a novel nerve conduit technology that has the potential to be optimized for greater functional restoration. "Successful regeneration" of a peripheral nerve injury is defined by the "re-establishment of targeted reinnervation with neurotransmission at the neuromuscular junction" and the "reversal of muscle fiber atrophy" (Deu-

mens et al., 2010). Compared to alternative surgical technologies available for nerve repair and regeneration following denervation, the utilization of the ENC led to the restoration of the neural pathway to the targeted tissue and the subsequent recovery of the function of the gastrocnemius muscle. Since the ENC is a biological fix, it avoids the bio-incompatibility issues observed with several of the synthetic conduits available on the market. The ENC allows for functional co-apting of the repair site and successful nerve cell migration and nerve tissue regeneration. In addition, the ENC can be fabricated from the patient's own cells eliminating immune rejection or the need for the harvesting of an autogenic nerve source. The ENC successfully eliminates many of the limitations observed with the commonly used conduit systems for nerve repair.

The utilization of ENCs in peripheral nerve repair may become more advantageous if the conduit itself is optimized in vitro. Conduit optimization may include the use of stem cells or neurotrophic factors within the conduit to act as growth cues for regenerating axons. This may increase the rate of regeneration of recovering axons, which would result in greater recovery of the targeted muscles. Furthermore, we are currently fabricating our ENCs from mesenchymal stem cells so that utilization of ENCs in a nerve repair surgery may provide an "off-the-shelf" technology as an alternative to nerve autografts.

Conflicts of interest: *None declared.*
Research ethics: *All animal care and animal surgeries were in accordance with the Guide for Care and Use of Laboratory Animals (Public Health Service, 19965, NIH Publication No. 85-23). The study protocol (09512) was approved by the University Committee for the Use and Care of Animals.*
Data sharing statement: *The datasets analyzed during the current study are available from the corresponding author on reasonable request.*
Plagiarism check: *Checked twice by iThenticate.*
Peer review: *Externally peer reviewed.*
Open peer review reports:
Reviewer 1: Muhammad Umer Nisar, University of Pittsburgh, USA.
Reviewer 2: Liancai Mu, Hackensack University Medical Center, USA.
Comments to authors: *This is a well written paper. However, further discussion should be made to clarify the advantages of ENC. The authors designed a study to evaluate the repair capabilities of their scaffoldless 3D engineered nerve conduits (ENC) as compared with those of engineered fibroblast conduits (EFC) and autografts in a 10-mm nerve gap in the tibial nerve of adult rats. The nerve gap resulted in denervation of both the medial and lateral gastrocnemius muscles. After 12 weeks, contractile properties of the gastrocnemius muscles and histology of muscle and nerve were examined to assess nerve regeneration and functional recovery. The*

authors reported that both ENCs and EFCs promoted neuronal regeneration in a 10-mm tibial nerve gap repair.
This study showed that autograft repair resulted in better axonal regeneration and force recovery as compared with ENC and EFC repairs. Further discussion is needed to show the advantages of the ENC over the EFC in nerve regeneration and functional restoration.
Recent studies have demonstrated that reinnervation of the denervated motor endplates in the target muscle is important for muscle reinnervation and functional recovery. It would be interesting to examine the alterations in motor endplates of the target muscle after ENC and EFC as well as autograft repair.

References

Akassoglou K, Yu WM, Akpinar P, Strickland S (2002) Fibrin inhibits peripheral nerve remyelination by regulating Schwann cell differentiation. Neuron 33:861-875.

Alluin O, Wittmann C, Marqueste T, Chabas JF, Garcia S, Lavaut MN, Guinard D, Feron F, Decherchi P (2009) Functional recovery after peripheral nerve injury and implantation of a collagen guide. Biomaterials 30:363-373.

Archibald SJ, Krarup C, Shefner J, Li ST, Madison RD (1991) A collagen-based nerve guide conduit for peripheral nerve repair: an electrophysiological study of nerve regeneration in rodents and nonhuman primates. J Comp Neurol 306:685-696.

Baltich J, Hatch-Vallier L, Adams AM, Arruda EM, Larkin LM (2010) Development of a scaffoldless three-dimensional engineered nerve using a nerve-fibroblast co-culture. In Vitro Cell Dev Biol Anim 46:438-444.

Bini TB, Gao S, Xu X, Wang S, Ramakrishna S, Leong KW (2004) Peripheral nerve regeneration by microbraided poly(L-lactide-co-glycolide) biodegradable polymer fibers. J Biomed Mater Res A 68:286-295.

Boyd JG, Gordon T (2003) Glial cell line-derived neurotrophic factor and brain-derived neurotrophic factor sustain the axonal regeneration of chronically axotomized motoneurons in vivo. Exp Neurol 183:610-619.

Brandt J, Dahlin LB, Lundborg G (1999) Autologous tendons used as grafts for bridging peripheral nerve defects. J Hand Surg Br 24:284-290.

Dalton PD, Flynn L, Shoichet MS (2002) Manufacture of poly(2-hydroxyethyl methacrylate-co-methyl methacrylate) hydrogel tubes for use as nerve guidance channels. Biomaterials 23:3843-3851.

Deumens R, Bozkurt A, Meek MF, Marcus MA, Joosten EA, Weis J, Brook GA (2010) Repairing injured peripheral nerves: Bridging the gap. Prog Neurobio 92:245-276.

Heine W, Conant K, Griffin JW, Hoke A (2004) Transplanted neural stem cells promote axonal regeneration through chronically denervated peripheral nerves. Exp Neurol 189:231-240.

Hudson TW, Evans GR, Schmidt CE (2000) Engineering strategies for peripheral nerve repair. Orthop Clin North Am 31:485-498.

Karacaoglu E, Yuksel F, Peker F, Guler MM (2001) Nerve regeneration through an epineurial sheath: its functional aspect compared with nerve and vein grafts. Microsurgery 21:196-201.

Kemp SW, Syed S, Walsh W, Zochodne DW, Midha R (2009) Collagen nerve conduits promote enhanced axonal regeneration, schwann cell association, and neovascularization compared to silicone conduits. Tissue Eng Part A 15:1975-1988.

Larkin LM, Calve S, Kostrominova TY, Arruda EM (2006) Structure and functional evaluation of tendon-skeletal muscle constructs engineered in vitro. Tissue Eng 12:3149-3158.

Lee AC, Yu VM, Lowe JB, 3rd, Brenner MJ, Hunter DA, Mackinnon SE, Sakiyama-Elbert SE (2003) Controlled release of nerve growth factor enhances sciatic nerve regeneration. Exp Neurol 184:295-303.

Lopatina T, Kalinina N, Karagyaur M, Stambolsky D, Rubina K, Revischin A, Pavlova G, Parfyonova Y, Tkachuk V (2011) Adipose-derived stem cells stimulate regeneration of peripheral nerves: BDNF secreted by these cells promotes nerve healing and axon growth de novo. PLoS One 6:e17899.

Lundborg G (2004) Alternatives to autologous nerve grafts. Handchir Mikrochir Plast Chir 36:1-7.

Lundborg G, Dahlin LB, Danielsen N, Hansson HA, Johannesson A, Longo FM, Varon S (1982) Nerve regeneration across an extended gap: a neurobiological view of nerve repair and the possible involvement of neuronotrophic factors. J Hand Surg Am 7:580-587.

Mahalingam VD, Behbahani-Nejad N, Ronan EA, Olsen TJ, Smietana MJ, Wojtys EM, Wellik DM, Arruda EM, Larkin LM (2015) Fresh versus frozen engineered bone-ligament-bone grafts for sheep anterior cruciate ligament repair. Tissue Eng Part C Methods 21:548-556.

Matsumoto K, Ohnishi K, Kiyotani T, Sekine T, Ueda H, Nakamura T, Endo K, Shimizu Y (2000) Peripheral nerve regeneration across an 80-mm gap bridged by a polyglycolic acid (PGA)-collagen tube filled with laminin-coated collagen fibers: a histological and electrophysiological evaluation of regenerated nerves. Brain Res 868:315-328.

Maurer K, Bostock H, Koltzenburg M (2007) A rat in vitro model for the measurement of multiple excitability properties of cutaneous axons. Clin Neurophysiol 118:2404-2412.

Meek MF, Varejao AS, Geuna S (2004) Use of skeletal muscle tissue in peripheral nerve repair: review of the literature. Tissue Eng 10:1027-1036.

Millesi H (1990) Progress in peripheral nerve reconstruction. World J Surg 14:733-747.

Millesi H (2007) Bridging defects: autologous nerve grafts. Acta Neurochir Suppl 100:37-38.

Murakami T, Fujimoto Y, Yasunaga Y, Ishida O, Tanaka N, Ikuta Y, Ochi M (2003) Transplanted neuronal progenitor cells in a peripheral nerve gap promote nerve repair. Brain Res 974:17-24.

Ray WZ, Mackinnon SE (2010) Management of nerve gaps: autografts, allografts, nerve transfers, and end-to-side neurorrhaphy. Exp Neurol 223:77-85.

Risitano G, Cavallaro G, Merrino T, Coppolino S, Ruggeri F (2002) Clinical results and thoughts on sensory nerve repair by autologous vein graft in emergency hand reconstruction. Chir Main 21:194-197.

Schlosshauer B, Dreesmann L, Schaller HE, Sinis N (2006) Synthetic nerve guide implants in humans: a comprehensive survey. Neurosurgery 59:740-747; discussion 747-748.

Schmidt CE, Leach JB (2003) Neural tissue engineering: strategies for repair and regeneration. Annu Rev Biomed Eng 5:293-347.

Taras JS, Nanavati V, Steelman P (2005) Nerve conduits. J Hand Ther 18:191-197.

Toba T, Nakamura T, Lynn AK, Matsumoto K, Fukuda S, Yoshitani M, Hori Y, Shimizu Y (2002) Evaluation of peripheral nerve regeneration across an 80-mm gap using a polyglycolic acid (PGA)--collagen nerve conduit filled with laminin-soaked collagen sponge in dogs. Int J Artif Organs 25:230-237.

Verdu E, Labrador RO, Rodriguez FJ, Ceballos D, Fores J, Navarro X (2002) Alignment of collagen and laminin-containing gels improve nerve regeneration within silicone tubes. Restor Neurol Neurosci 20:169-179.

Wang S, Wan AC, Xu X, Gao S, Mao HQ, Leong KW, Yu H (2001) A new nerve guide conduit material composed of a biodegradable poly(phosphoester). Biomaterials 22:1157-1169.

Wood MD, Hunter D, Mackinnon SE, Sakiyama-Elbert SE (2010) Heparin-binding-affinity-based delivery systems releasing nerve growth factor enhance sciatic nerve regeneration. J Biomater Sci Polym Ed 21:771-787.

Wood MD, Moore AM, Hunter DA, Tuffaha S, Borschel GH, Mackinnon SE, Sakiyama-Elbert SE (2009) Affinity-based release of glial-derived neurotrophic factor from fibrin matrices enhances sciatic nerve regeneration. Acta Biomater 5:959-968.

Yang Y, Ding F, Wu J, Hu W, Liu W, Liu J, Gu X (2007) Development and evaluation of silk fibroin-based nerve grafts used for peripheral nerve regeneration. Biomaterials 28:5526-5535.

Zuo J, Neubauer D, Graham J, Krekoski CA, Ferguson TA, Muir D (2002) Regeneration of axons after nerve transection repair is enhanced by degradation of chondroitin sulfate proteoglycan. Exp Neurol 176:221-228.